Supplementary Material

Dimeric BODIPY-loaded liposomes for dual hypoxia markers imaging and activatable photodynamic therapy against tumor

Huachao Chen, Qirui Bi, Yongrong Yao, Ninghua Tan *

State Key Laboratory of Natural Medicines, Jiangsu Key Laboratory of TCM Evaluation and Translational Research, School of Traditional Chinese Pharmacy, China Pharmaceutical University, Nanjing 211198, China.

*Corresponding author, Ninghua Tan, Email: nhtan@cpu.edu.cn

Supplementary figures

1. **Scheme S1.** Synthesis of DiBDP.
2. **Fig. S1.** ^{1}H NMR spectrum of DiBDP in $CDCl_3$.
3. **Fig. S2.** ^{13}C NMR spectrum of DiBDP in $CDCl_3$.
4. **Fig. S3.** MS HRMS (TOF-ESI) spectrum of DiBDP.
5. **Fig. S4.** UV-VIS-NIR absorption spectrum of DiBDP in $CHCl_3$.
6. **Fig. S5.** Long-term-stability study of Ab-DiBDP NPs in RPMI 1640 with 10% FBS, DMEM with 10% FBS, or PBS.
7. **Fig. S6.** TEM micrographs of Ab-DiBDP NPs in water.
8. **Fig. S7.** In vitro release profiles of DiBDP from Ab-DiBDP NPs at pH 7.4, 6.0 and 5.0. Data are means ± SD (n = 3).
9. **Fig. S8.** Co-localization images of Ab-DiBDP NPs in HeLa cells.
10. **Fig. S9.** Confocal fluorescence images of HeLa cells cultured under normoxic (20% pO_2) or hypoxic (3% and 1% pO_2) conditions for 6 h with different treatments after irradiation: Ab-DiBDP NPs + SOSG; NAC + Ab-DiBDP NPs + SOSG.
11. **Fig. S10.** The body weight variation of tumour-bearing mice during treatment.
12. **Fig. S11.** Survival rates of tumor-bearing mice with different treatments indicated (n = 6).
13. **Fig. S12.** H&E stained images of tissue sections from different organs of mice after Ab-DiBDP NPs-mediated PDT and the age-matched healthy mice without treatment (control).

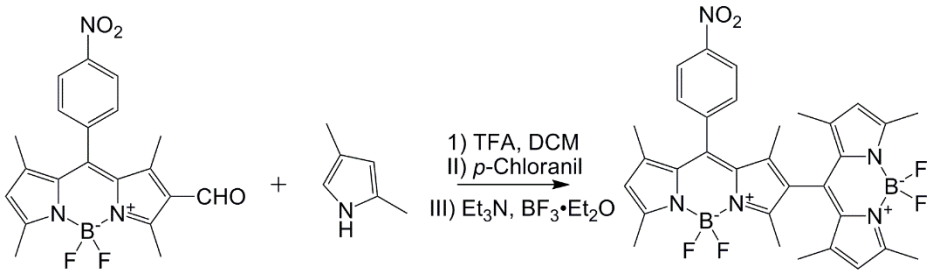

Scheme S1. Synthesis of DiBDP.

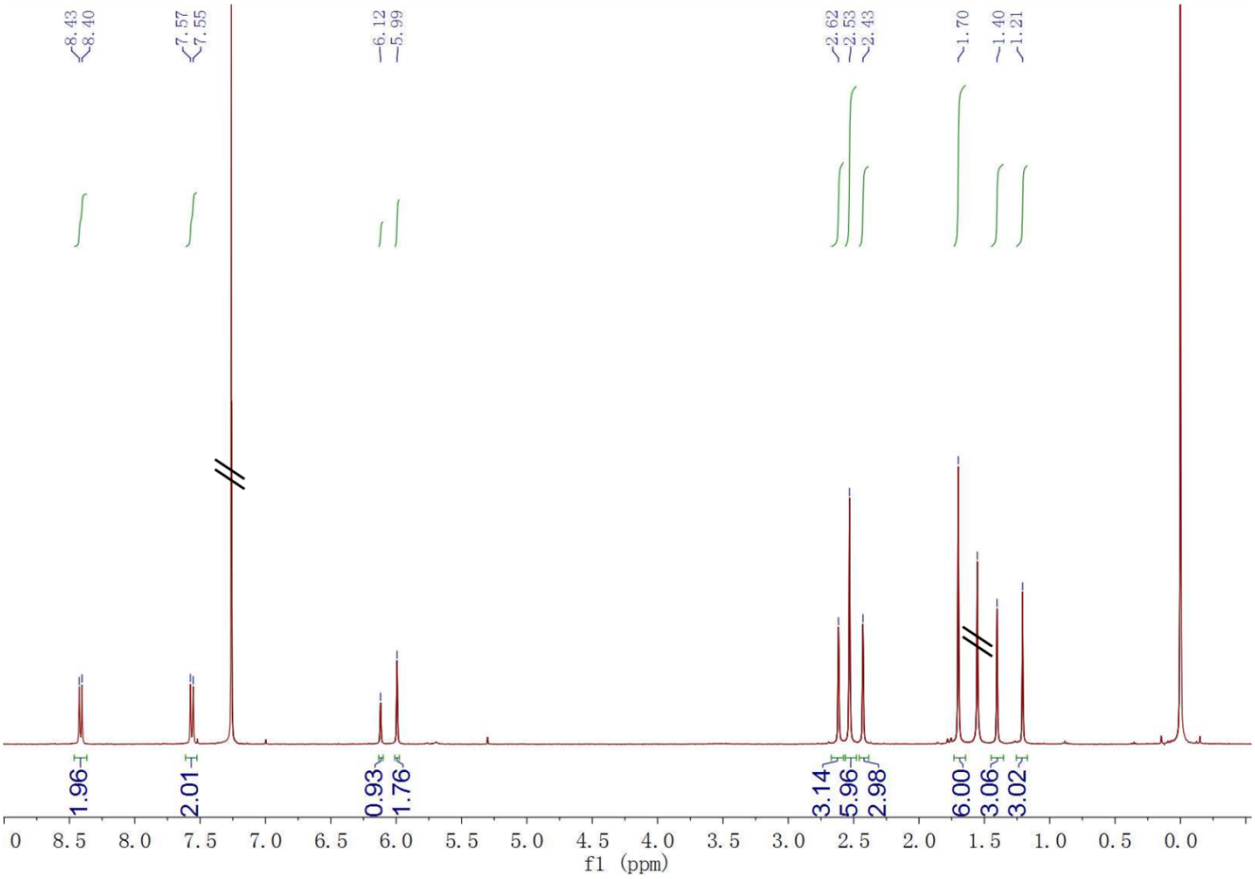

Fig. S1. ^{1}H NMR spectrum of DiBDP in $CDCl_3$.

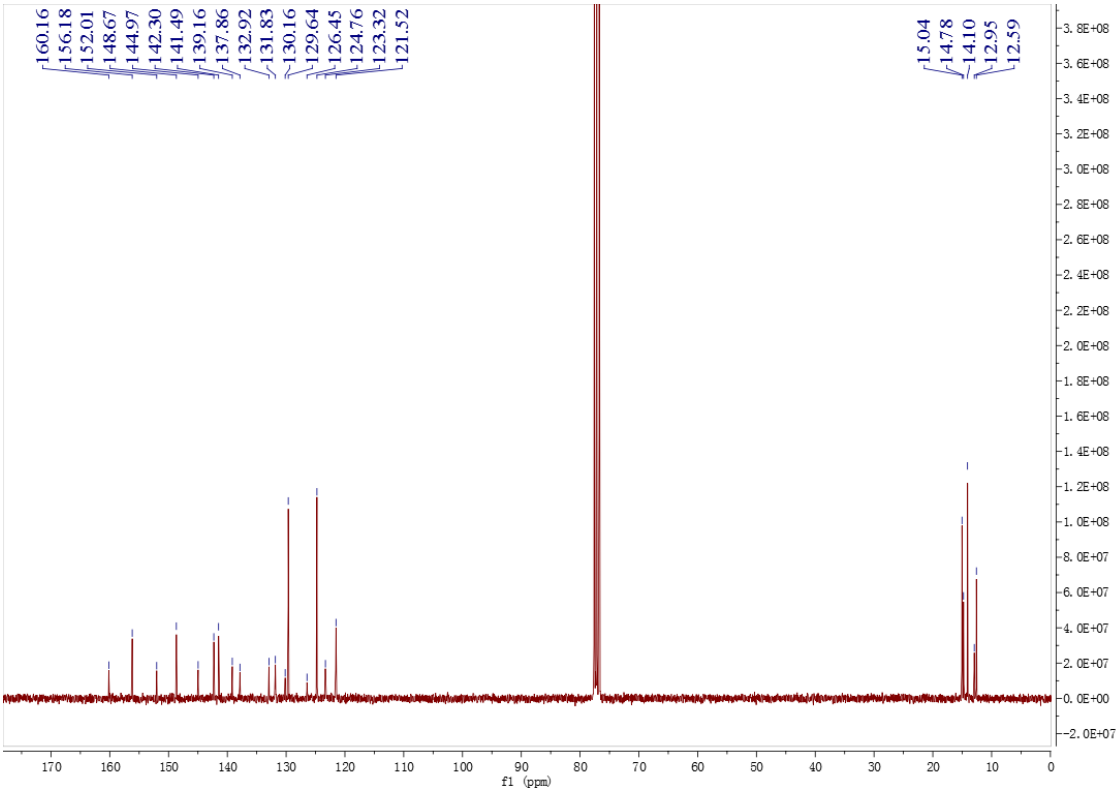

Fig. S2. ^{13}C NMR spectrum of DiBDP in $CDCl_3$.

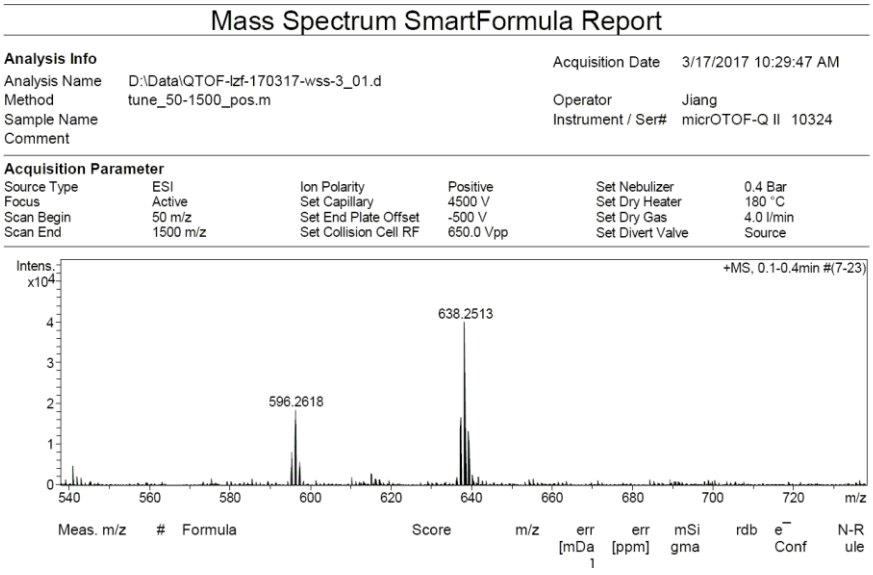

Fig. S3. MS HRMS (TOF-ESI) spectrum of DiBDP.

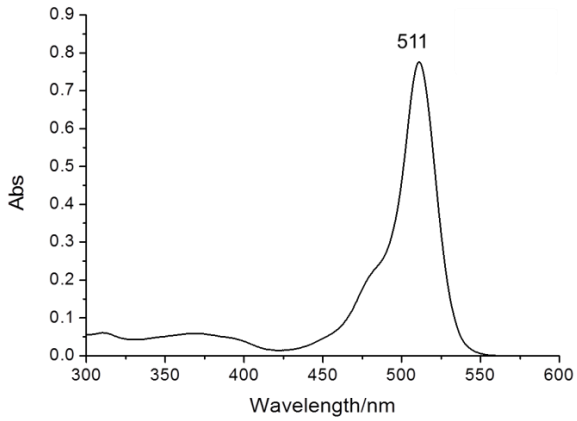

Fig. S4. UV-VIS-NIR absorption spectrum of DiBDP in $CHCl_3$.

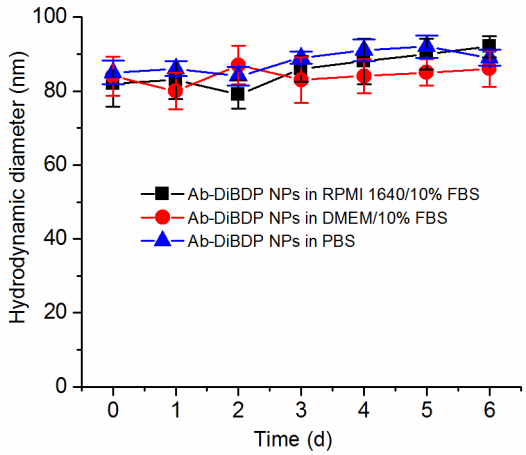

Fig. S5. Long-term-stability study of Ab-DiBDP NPs in RPMI 1640 with 10% FBS, DMEM with 10% FBS, or PBS.

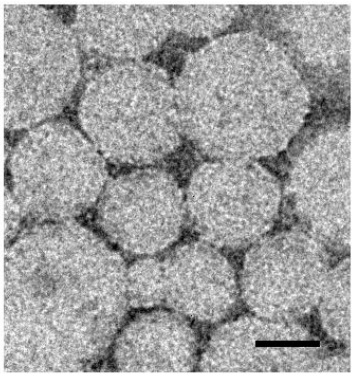

Fig. S6. TEM micrographs of Ab-DiBDP NPs in water. Scale bar = 50 nm.

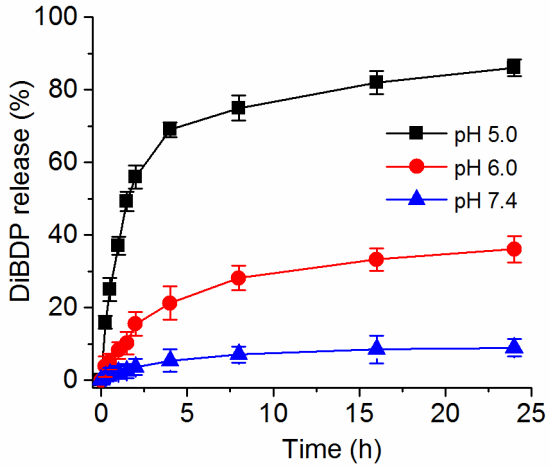

Fig. S7. In vitro release profiles of DiBDP from Ab-DiBDP NPs at pH 7.4, 6.0 and 5.0. Data are means ± SD (n = 3).

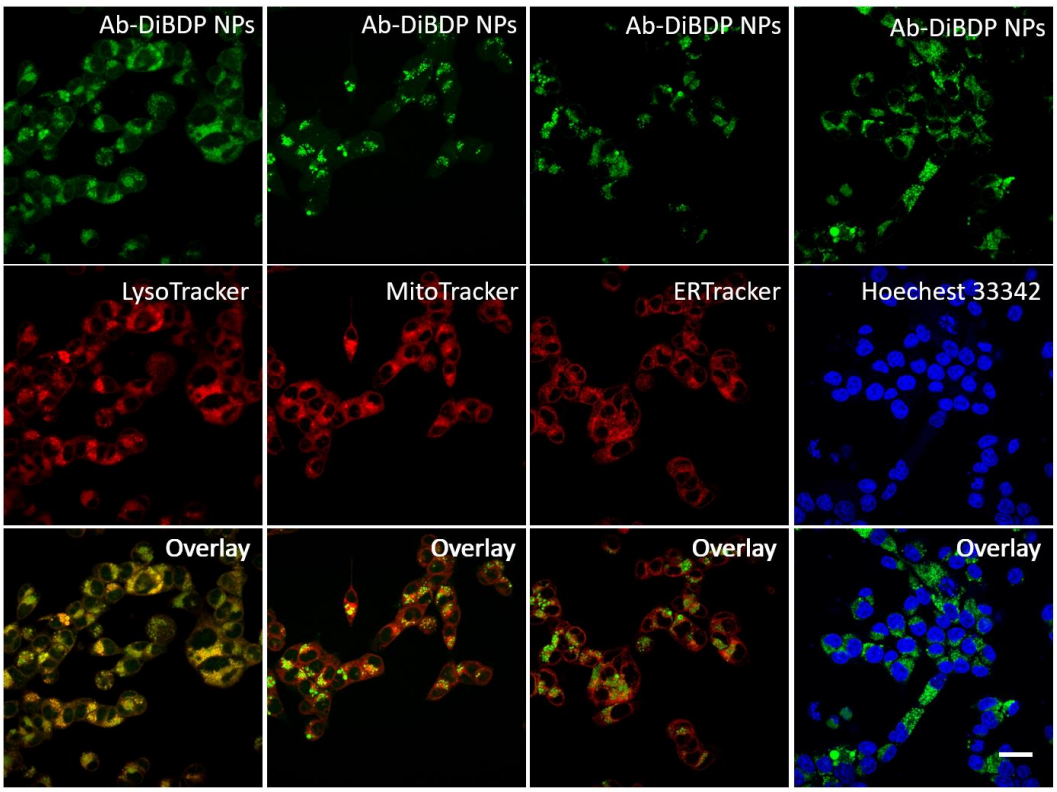

Fig. S8. Co-localization images of Ab-DiBDP NPs in HeLa cells. HeLa cells were incubated with Ab-DiBDP NPs at 37 °C for 1 h, and then incubated with 100 nM LysoTracker Blue, ER Tracker Blue, Hoechst 33342 and MitoTracker Blue 10 min. Scale bar = 40 μm.

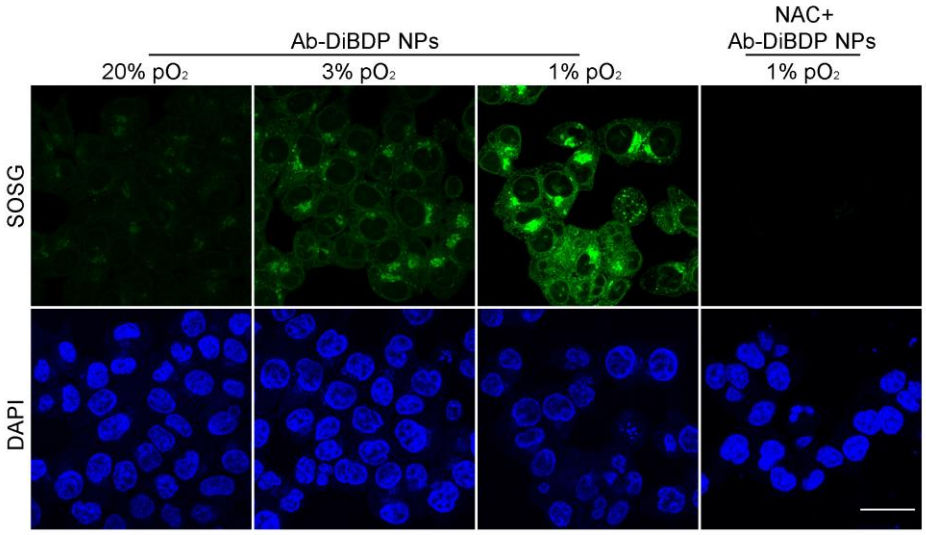

Fig. S9. Confocal fluorescence images of HeLa cells cultured under normoxic (20% pO_2) or hypoxic (3% and 1% pO_2) conditions for 6 h with different treatments after irradiation: Ab-DiBDP NPs + SOSG; NAC + Ab-DiBDP NPs + SOSG. Scale bar = 40 μm.

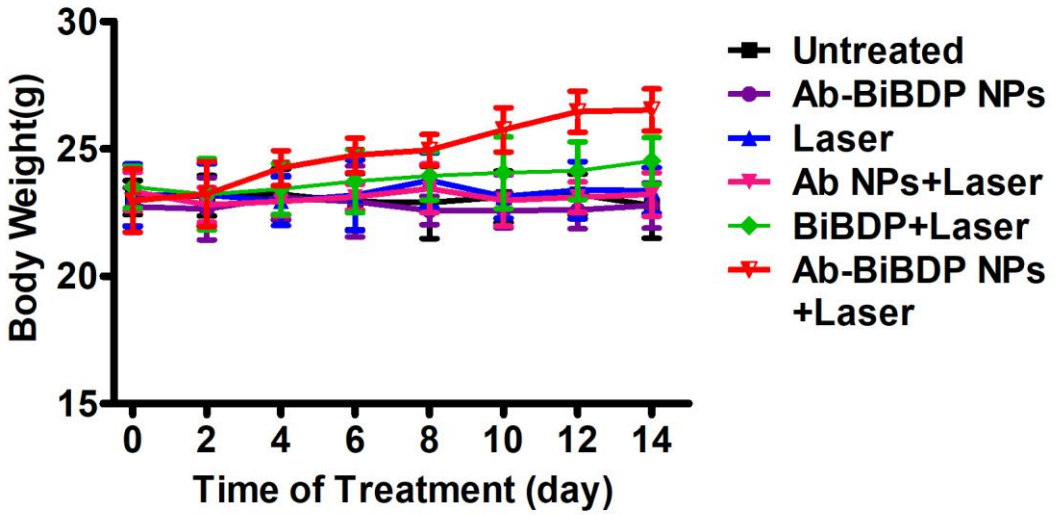

Fig. S10. The body weight variation of tumour-bearing mice during treatment.

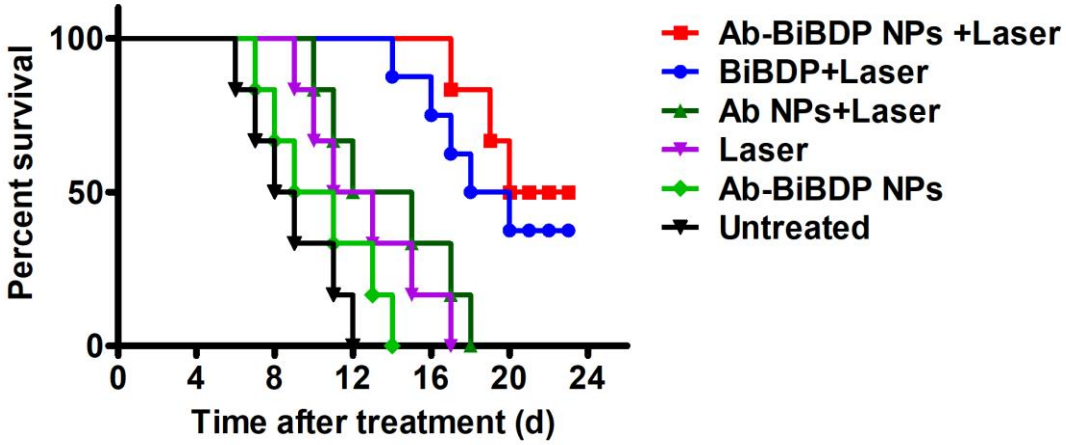

Fig. S11. Survival rates of tumor-bearing mice with different treatments indicated (n = 6).

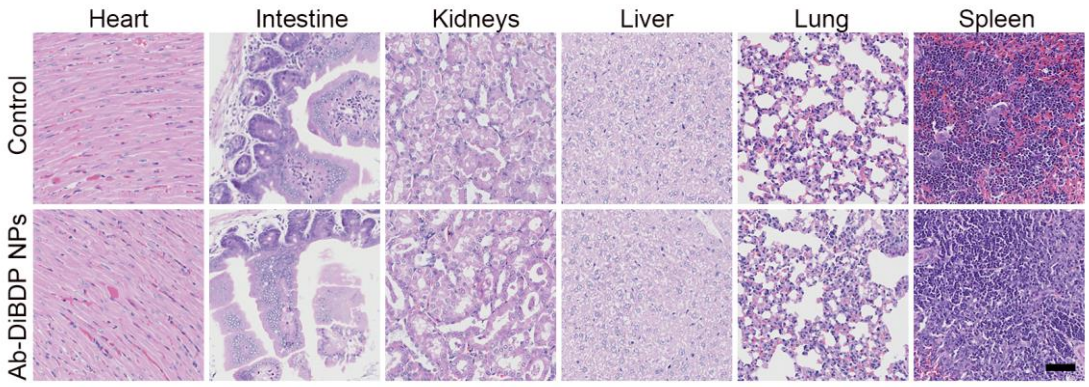

Fig. S12. H&E stained images of tissue sections from different organs of mice after Ab-DiBDP

NPs-mediated PDT and the age-matched healthy mice without treatment (control). Scale bar = 100 μm.